

Atmospheric Degradation of Cyclic Volatile Methyl Siloxanes: Radical Chemistry and Oxidation Products

Mitchell W. Alton and Eleanor C. Browne*

Cite This: *ACS Environ. Au* 2022, 2, 263–274

Read Online

ACCESS |



Metrics & More



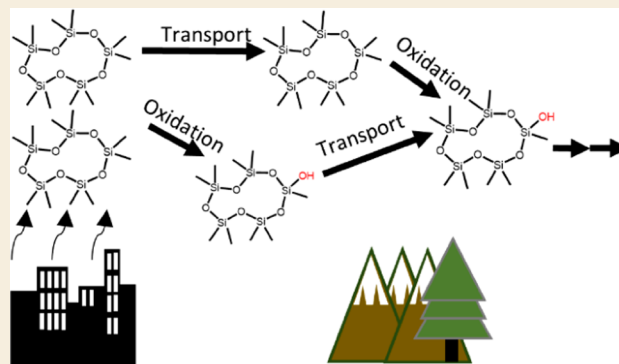
Article Recommendations



Supporting Information

ABSTRACT: Cyclic volatile methyl siloxanes (cVMS) are anthropogenic chemicals that have come under scrutiny due to their widespread use and environmental persistence. Significant data on environmental concentrations and persistence of these chemicals exists, but their oxidation mechanism is poorly understood, preventing a comprehensive understanding of the environmental fate and impact of cVMS. We performed experiments in an environmental chamber to characterize the first-generation oxidation products of hexamethylcyclotrisiloxane (D3), octamethylcyclotetrasiloxane (D4), and decamethylcyclopentasiloxane (D5) under different peroxy radical fates (unimolecular reaction or bimolecular reaction with either NO or HO₂) that approximate a range of atmospheric compositions. While the identity of the oxidation products from D3 changed as a function of the peroxy radical fate, the identity and yield of D4 and D5 oxidation products remained largely constant. We compare our results against the output from a kinetic model of cVMS oxidation chemistry. The reaction mechanism used in the model is developed using a combination of previously proposed cVMS oxidation reactions and standard atmospheric oxidation radical chemistry. We find that the model is unable to reproduce our measurements, particularly in the case of D4 and D5. The products that are poorly represented in the model help to identify possible branching points in the mechanism, which require further investigation. Additionally, we estimated the physical properties of the cVMS oxidation products using structure–activity relationships and found that they should not be significantly partitioned to organic or aqueous aerosol. The results suggest that cVMS first-generation oxidation products are also long-lived in the atmosphere and that environmental monitoring of these compounds is necessary to understand the environmental chemistry and loading of cVMS.

KEYWORDS: VMS, siloxanes, atmospheric oxidation, peroxy radical, oxidized VMS, contaminants of emerging concern



1. INTRODUCTION

Cyclic volatile methyl siloxanes (cVMS) are high-production volume chemicals^{1,2} that are common components of consumer and industrial products such as deodorants, lotions, sealants, and lubricants. cVMS have high vapor pressures and low Henry's solubilities, leading to preferential partitioning into the atmosphere³ where they primarily degrade through reactions with OH.⁴ cVMS lifetimes with respect to oxidation by OH are between 4 and 10 days (assuming a 24 h average OH concentration of 1.2×10^6 molecules cm⁻³),^{4–12} and consequently, cVMS are globally distributed and have been identified in remote environments such as the arctic.^{13–15} These abundant chemicals are also bioaccumulative and toxic.^{13,16–18} Consequently, the European Union placed restrictions on the use of cVMS in certain cosmetic products in 2016, with recommendations in 2021 to restrict the use in certain industrial processes.^{19–21} Owing to their widespread use, toxicity, and environmental persistence, there has been significant interest in understanding the environmental fate of cVMS.^{5,12,13,16,17,22–38}

Previous research has largely focused on quantifying ambient concentrations of parent cVMS^{13,23,26,39} and understanding their oxidation kinetics,^{5,10,11} significantly less is understood about the identity of cVMS oxidation products and their environmental chemistry.^{36,37} In the atmosphere, cVMS oxidation is initiated by reactions with OH or Cl to produce an alkyl radical (R₃SiCH₂•), which quickly reacts with O₂ to produce a peroxy radical (R₃SiCH₂O₂•, or more generally, RO₂). The subsequent reactions depend on atmospheric composition: reactions with NO will dominate under high NO mixing ratios, such as in urban areas; reactions with HO₂ will dominate where high HO₂ mixing ratios are found, such as in areas dominated by biogenic emissions; and unimolecular

Received: October 16, 2021

Revised: February 3, 2022

Accepted: February 4, 2022

Published: February 17, 2022



Table 1. Radical Precursor Concentrations, Estimated Oxidant Concentrations, and Estimated Ratios of the Reaction between RO₂ and NO to HO₂ and HO₂ to other RO₂

cVMS ^a	oxidant precursor and concentration (ppb _v) ^b	[OH] or [Cl] (molecules cm ⁻³)	[NO], [NO ₂] (ppb)	NO/HO ₂ ^c	τ _{RO₂} (s) ^d
D3* ^e	Cl ₂ , 15	1.0 × 10 ⁶		0.4:1	27
D3*	H ₂ O ₂ , 1000	8.0 × 10 ⁷		0.04:1	4
D3*	HONO, 400	5.0 × 10 ⁷	200,150	200:1	0.02
D3	Cl ₂ , 15	1.0 × 10 ⁶		0.4:1	27
D4	Cl ₂ , 15	6.0 × 10 ⁵		0.9:1	40
D4	H ₂ O ₂ , 1000	8.0 × 10 ⁷	0.05, 8	0.04:1	4
D4	HONO, 400	5.0 × 10 ⁷	230,190	100:1	0.02
D4	Cl ₂ , 100 CH ₂ O, 1000	7.0 × 10 ⁵		0.02:1	1.6
D5	Cl ₂ , 15	4.0 × 10 ⁵	0.05, 0.05	1:1	46
D5	H ₂ O ₂ , 1000	8.0 × 10 ⁷	0.05, 4	0.04:1	4
D5	HONO, 400	5.0 × 10 ⁷	250,180	100:1	0.02

^aApproximately 80 ppb_v of cVMS was added to the chamber. ^bThe initial mixing ratios of NO and NO₂ before the lights were turned on in HONO experiments were ~50 and ~100 ppb_v, respectively, except for D3, which had ~100 ppb_v of NO. Differences in mixing ratios are due to the inconsistency of HONO generation using HNO₃ and NaNO₂. NO and NO₂ were only measured in experiments for which mixing ratios are reported. For other experiments, background mixing ratios of 50 ppt_v were assumed. ^cEstimated radical concentrations were determined at the point that 10% of the cVMS has reacted, as calculated from the KinSim model. ^dRate constants used in calculating the RO₂ lifetimes were obtained from Ziemann and Atkinson: ⁴⁶ $k_{\text{RO}_2+\text{HO}_2} = 1.5 \times 10^{-11}$ molecules cm⁻³ s⁻¹, $k_{\text{RO}_2+\text{NO}} = 9 \times 10^{-12}$ molecules cm⁻³ s⁻¹, $k_{\text{RO}_2+\text{RO}_2} = 1 \times 10^{-14}$ molecules cm⁻³ s⁻¹, and $k_{\text{RO}_2+\text{OH}/\text{Cl}} = 2 \times 10^{-10}$ molecules cm⁻³ s⁻¹. ^eExperiments marked with (*) were performed in semibatch mode, in which sampled air is continually replaced with clean air to maintain a constant chamber volume for the duration of the experiment.

reactions can dominate in areas with low mixing ratios of NO or HO₂, such as remote regions or even in urban areas for reactions with sufficiently fast unimolecular reactions.⁴⁰

Laboratory investigations of cVMS oxidation have observed numerous oxidation products but typically identify siloxanol (–CH₃ replaced with –OH) as the main product.^{4,7,8} Two experimental studies have also reported the formate ester (–CH₃ replaced with –CH(O)H) product.^{4,5} Additionally, oxidation products such as hydroperoxides, alcohols (R₃SiCH₂OH), and products with an increased number of silicon atoms have been detected.^{8,41} Siloxanol formation has often been ascribed to the hydrolysis of formate ester,^{4,7} a process that likely occurs on surfaces. Attempts to develop an oxidation mechanism based on these observations and known atmospheric peroxy radical chemistry have largely been unsuccessful, in part, because the RO₂ fate has been unclear in many of the past experiments. It has generally been concluded that Si in cVMS allows for unique chemistry to occur and several unusual reactions have been proposed based on the laboratory results.^{4,8,18} Recent theoretical investigations of organosilicon chemistry provide evidence that organosilicon compounds undergo unique rearrangements inaccessible to carbon-based compounds.^{36,37} The net effect of the mechanism proposed by the theoretical investigations oxidation under high NO_x (=NO + NO₂) conditions includes the production of HO₂ and the oxidation of two NO radicals to NO₂.^{36,37} This net effect is inconsistent with laboratory measurements showing that at most one NO is oxidized to NO₂ during cVMS oxidation and that cVMS reduces O₃ production and OH radical concentrations.¹⁸ However, as cVMS oxidation products were not measured, there is still an opportunity for better online characterization of the chemistry.

Without an understanding of the cVMS oxidation mechanism and products, it is difficult to predict the fate of the oxidation products. For instance, one possibility is that the oxidation products contribute to aerosol mass. Based on observations of Si in urban nanoparticles, it has been suggested that oxidation products of cVMS from personal care products are present in aerosol,^{29,39,42} while other studies have

suggested that silicon in aerosol from organosilicon compounds is minimal.^{43,44} There are substantial variations in the reported aerosol yields of cVMS, which range from approximately 0–50%.⁴⁵ The range in the reported yields is likely due to experimental conditions creating different oxidation products. Without knowledge of the oxidation mechanism and measurements of the oxidation products, however, this hypothesis is difficult to test.

In this study, we conducted a series of atmospheric chamber experiments designed to investigate the reaction mechanisms of hexamethylcyclotrisiloxane (D3), octamethylcyclotetrasiloxane (D4), and decamethylcyclopentasiloxane (D5) under conditions of different RO₂ lifetimes and reaction partners. We also oxidized fully deuterated hexamethyldisiloxane (D₁₈L2) with Cl atoms to provide some constraint on the identity of the oxidation products. Using a combination of our measurements, kinetic modeling, and constraints from the literature, we propose a simplified oxidation mechanism for cVMS that can be used in modeling atmospheric cVMS chemistry. We identify points in the cVMS oxidation mechanism that require further investigation. The environmental fate of the observed products is investigated through estimations of vapor pressure and water solubility, with the results suggesting that the first generation of cVMS oxidation does not create oxidation products that will participate in aerosol growth.

2. MATERIALS AND METHODS

Experiments were performed in a ~1 m³ FEP Teflon chamber at ambient lab temperature (295 ± 3 K) and pressure (~860 mbar) at low relative humidity (<5% RH). A low RH was used to minimize the wall loss of the oxidation products. The chamber, previously described in Alton and Browne,⁵ was run in either batch mode, in which the chamber was slowly collapsed as air was sampled from it, or semibatch mode, in which the sampled air was continuously replaced. To correct for dilution in semibatch mode, the dilution rate was quantified by sampling for 30 min after completion of the experiment and determining the first-order loss constant for each product. This rate constant represents both loss to the walls and dilution and was used to correct the measured values for individual species. Experiments for D3

were conducted in both batch and semibatch modes and product distributions were determined to be consistent between the two methods of chamber operation on the timescale we are interested in (~ 3 h). Experimental conditions are summarized in Table 1.

D3 (98%, Acros Organics), D4 (98%, Acros Organics), D5 (97%, Sigma-Aldrich) were diluted in acetonitrile (99.8%, Sigma-Aldrich) to 5% (w/w) and injected into the chamber using a gently heated borosilicate glass tube with a stream of zero-air (AADC0 Instruments, 737 series) transporting the evaporated cVMS to the chamber. We saw no evidence for thermal degradation of the cVMS from heating of the tube (maximum temperature estimated at less than 60 °C). The oxidation chemistry of each precursor was investigated under three different RO₂ fates. Peroxy radical lifetimes were calculated using measured concentrations of NO or estimated concentrations of reactive species from a kinetic model, which will be discussed later in Section 3.3. Experiments using Cl₂ as an oxidant precursor were designed to favor unimolecular RO₂ reactions. For these experiments, we calculate a RO₂ lifetime with respect to bimolecular reactions of about 0.4 min with $\sim 55\%$ of the RO₂ reacting with HO₂ and 20% undergoing unimolecular rearrangements (assuming a rate constant of $8 \times 10^{-3} \text{ s}^{-1}$ for isomerization),³⁶ and the rest reacting with background NO. Experiments using H₂O₂ as an oxidant precursor probed conditions where $>90\%$ of RO₂ react with HO₂, while experiments using HONO resulted in $\sim 99\%$ of RO₂ reacting with NO.

Cl₂ was added by a flow of N₂ over a gravimetrically calibrated permeation device (VICI Metronics). Hydrogen peroxide was added via a solution added into the heated borosilicate glass tube with a zero-air flow. HONO was generated by the addition of 40 μL of a 1.5 M sodium nitrite solution ($>99\%$, Sigma-Aldrich) to a 2 M nitric acid solution (70%, Fischer Scientific) while passing zero-air over the headspace of the solution, transporting any evolved gases into the chamber. Cl₂ and HONO were photolyzed into Cl atoms and OH + NO, respectively, with 370 nm fluorescent lights (General Electric, F40BL) positioned below the chamber. H₂O₂ was photolyzed with 254 nm lights (General Electric, G36T8) to generate OH. Control experiments were performed to ensure the parent cVMS were stable in the presence of UV light. To test for photostability of hydroperoxides generated from D4 oxidation, we performed a control experiment where we photolyzed Cl₂ with 370 nm lights with ~ 1 ppm_v of added formaldehyde to generate HO₂. Partway through the experiment, 254 nm lights were also turned on with 370 nm lights. The production of hydroperoxides increased at the same rate as siloxanol, suggesting that more Cl₂ was photolyzed with the additional lights increasing total oxidation, but there was no additional loss of the hydroperoxide from photolysis.

As in our previous work,⁵ a high-resolution long time-of-flight chemical ionization mass spectrometer (CIMS; Aerodyne Research, Inc. and ToFwerk AG; resolving power $\sim 8000 \text{ m/z}/\Delta\text{m/z}$) using protonated toluene as the reagent ion measured the cVMS parent compounds and oxidation products during the experiments. Compounds are detected as $[\text{M} + \text{H}]^+$ products. The ionization is relatively soft; we do not detect the methane fragment (R_3Si^+) from the parent cVMS that is generally seen in other proton-transfer ionization schemes. We did observe R_3Si^+ as a fragment of the siloxanol product, though less than 3% of the siloxanol signal was detected as this fragment. The CIMS sampled a total of 1.7 slpm, with 700 sccm of that flow consisting of humidified zero-air and the rest sampled from the chamber. The addition of water vapor enhances the instrument response (counts per second per ppb_v normalized to the toluene reagent ion signal; ncps) for detection of cVMS and the oxidation products. Data was postprocessed in ToFwerk v3.2.3 (ToFwerk AG) in the IGOR Pro environment (Wavemetrics, v8.0.4.2) using fully constrained peak fitting and allocation of isotope signals. An example of the peak fitting is shown in Section S1 of the Supporting Information (Figure S1). NO and NO₂ concentrations were measured using a chemiluminescence NO and NO₂ analyzer with a blue light converter for true NO₂ measurements (Teledyne, T200UP) with 1 min resolution and 50 ppt_v limit of detection.

We used KinSim v4.14⁴⁷ in Igor Pro to simulate gas-phase chemistry for each experiment. KinSim is an open-source solver for kinetics modeling. Rate constants for non-cVMS species were obtained from Atkinson et al.⁴⁸ and Atkinson.⁴⁹ The mechanism used in the KinSim simulations is presented in Section S2 of the Supporting Information. The lifetime of cVMS species with respect to oxidation by OH (\sim days) requires the use of elevated radical concentrations to ensure sufficient oxidation on the timescale of our experiment. However, the experiments were designed to avoid potentially unrepresentative reactions in the atmosphere (such as RO₂ + RO₂ or RO₂ + OH). We assumed that the chamber was well mixed. Wall-partitioning calculations for all cVMS products were included using KinSim's built-in wall-partitioning functions.⁵⁰ The reversible vapor–wall interactions were calculated upon mechanism compilation using the first-order vapor condensation rate coefficient ($1 \times 10^{-3} \text{ s}^{-1}$),⁵¹ the mass vapor saturation concentration of the partitioning molecule, and enthalpy of vaporization, with the latter two values estimated by the melting point, boiling point, and vapor pressure module (MPBPWIN v1.44) in the Environmental Protection Agency's (EPA) Estimations Programs Interface for Windows (EPIWIN v4.11). Rate constants for peroxy radical reactions with NO and HO₂ were taken from Atkinson and Ziemann⁴⁶ and were kept constant. As the oxidation rate constants for the different parent cVMS are known,⁵ the decay of the cVMS was used to constrain the concentration of oxidants, which was then used to determine the photolysis rates of the oxidant precursors. An average photolysis rate was used for all experiments using the same oxidant precursor (7×10^{-5} , 2×10^{-4} , and $4 \times 10^{-4} \text{ s}^{-1}$ for H₂O₂, Cl₂, and HONO, respectively).

For estimating partitioning between condensed phases in the atmosphere, we used EPIWIN to calculate the water solubility with the Water Solubility and Octanol-Water Partition Coefficient (WSKOW v1.43) and the Henry's law constant with the HenryWin v3.21 module. In addition to EPIWIN, the EPA's Toxicity Estimation Software Tool (TEST) was used to estimate the vapor pressures, boiling points, and water solubilities of the cVMS and their oxidation products. TEST does not estimate Henry's Law constants; however, a proxy of the ratio between the vapor pressure and the water solubility of the compound can be used to compare between the EPIWIN and TEST.⁵² TEST reports a consensus value where it estimates the values using multiple methods then averages those results together. These estimations are further discussed in Section 3.4.

3. RESULTS AND DISCUSSION

3.1. cVMS Oxidation Products

Figure 1 shows an example time series from a D3 oxidation experiment with H₂O₂ as the oxidant precursor. The only product to exhibit significant loss after the lights are turned off is the difunctional siloxanol + formate ester product. As oxidants are continuously generated during these experiments, the first-generation oxidation products will undergo further oxidation. To minimize the impact of this oxidation, we analyze the product signals at the point where only 10% of the parent cVMS has been oxidized. This metric was chosen as only 4% of the oxidation products are expected to have reacted at this point due to the continued generation of oxidants. Additionally, although the oxidation products are expected to have lifetimes with respect to wall loss greater than 1 h, measuring the products after only 10% of the cVMS reacted (~ 30 min) minimizes the impacts of wall loss on the measured concentrations. Comparing the results at the point where 10% of the cVMS has reacted allows for an easier intercomparison between the different experiments, as we are achieving the same oxidant exposures.

Possible isomers of select D3 oxidation products are shown in Figure 2. These assignments are proposed based on previous

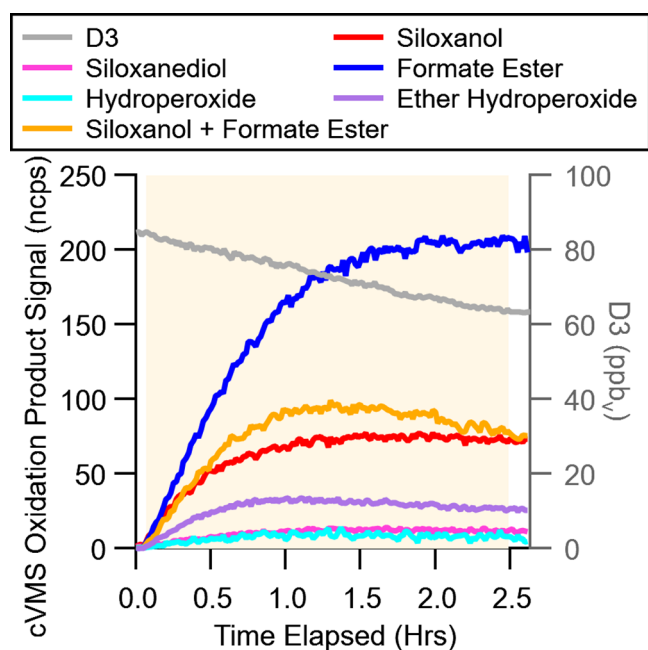


Figure 1. Example time series of D3 oxidation with H_2O_2 as oxidant precursors. The shading signifies when the lights are on, and the dashed vertical line signifies when 10% of D3 had been oxidized. Signals averaged to 1 min time resolution are shown.

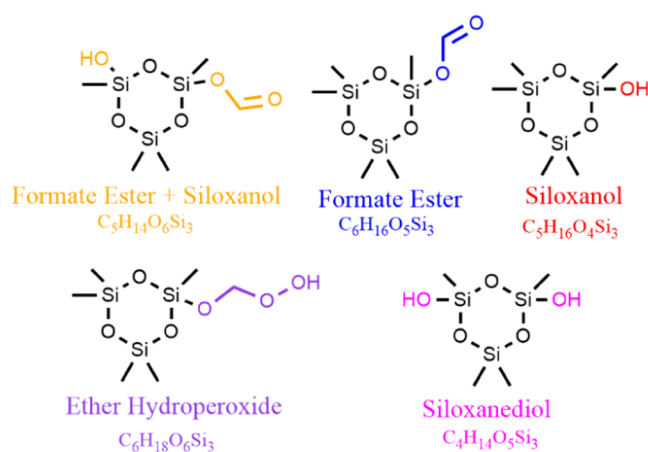


Figure 2. Example cVMS oxidation product structures.

works^{4,7,8} and further informed through isotopically labeled linear VMS experiments (described in Section S3 of the Supporting Information). We did not detect the formation of any oxidation products that contained either fewer or greater silicon atoms than the parent compound. For instance, we did not observe the formation of either D4 or a product with 10 silicon atoms during the oxidation of D5.

The CIMS was calibrated for the parent siloxanes. The sensitivity to the parent compounds in these experiments was lower than reported in previous works⁵ as the ion optics were tuned for optimal resolving power, which sacrificed sensitivity. Authentic standards for cVMS oxidation products are not commercially available, and thus, we are unable to quantify their concentrations. However, after normalization to the reagent ion and when working in the linear response region, the instrument response to a specific compound will be linear with respect to changes in concentration. As the reagent ion exhibited no significant depletion and signals were significantly

above the limit of detection, these experiments are within the linear response region. Thus, although the oxidation products cannot be quantified, differences across RO_2 fate conditions in the signal of a given product can be interpreted as changes in the relative amount of a product being formed. Moreover, as shown in Section S4 of the Supporting Information, when 10% of the cVMS had reacted, the total signal of the oxidation products detected normalized to the mixing ratio of cVMS reacted, varied by <20% across the experimental conditions (Figures S3 and S4) even when there are significant changes in the compositions of the ions formed (particularly for D3). This finding suggests that variations in instrument response to different products were relatively small and that we were capturing most of the oxidation products.

Given the absence of authentic calibration standards, we elect to report the product abundance in terms of the normalized signal yield. This quantity is calculated as the signal of an individual product divided by the sum of the total product signals and would be approximately equal to the molar yield if we had equal sensitivity to every oxidation product. Figure 3 shows the normalized signal yields of each of the products for the different cVMS studied.

The oxidation mechanism of D3 has been studied with theoretical calculations and will be discussed first. The most intense product signal formed in the D3 experiments under conditions that favored unimolecular reactions, as seen in Figure 3c, was $(\text{C}_5\text{H}_{14}\text{O}_6\text{Si}_3)\text{H}^+$. We assign this formula as a difunctional product: siloxanol and formate ester. In the $\text{RO}_2 + \text{NO}$ and $\text{RO}_2 + \text{HO}_2$ conditions, the product with the most intense signal was $(\text{C}_6\text{H}_{16}\text{O}_5\text{Si}_3)\text{H}^+$, which corresponds to the formate ester product. The next most intense signal in the experiments was $(\text{C}_5\text{H}_{16}\text{O}_4\text{Si}_3)\text{H}^+$, which we identified as siloxanol. We attribute $(\text{C}_6\text{H}_{18}\text{O}_6\text{Si}_3)\text{H}^+$ to an ether hydroperoxide and $(\text{C}_6\text{H}_{18}\text{O}_5\text{Si}_3)\text{H}^+$ to the hydroperoxide. The hydroperoxide was identified by Sommerlade et al.,⁸ though the ether hydroperoxide was not. No nitrogen-containing peaks were identified when D3 was oxidized in high NO_x (~ 100 ppbv NO_x) conditions. This observation may suggest that the formation of organic nitrates was unfavorable. Alternatively, organic nitrates may be detected with low efficiency because of either fragmentation or low ionization efficiency. The presence of and instrument response to organic nitrates will be discussed further in the context of D4 and D5 oxidation.

The assignment of $(\text{C}_6\text{H}_{16}\text{O}_5\text{Si}_3)\text{H}^+$ as a formate ester rather than a carboxylic acid was informed by previous experimental and theoretical work.^{4,37} Additionally, we oxidized fully deuterated hexamethyldisiloxane (D_{18}L_2) with Cl atoms in a similar experiment to Atkinson et al.⁴ and observed $(\text{C}_6\text{D}_{16}\text{O}_5\text{Si}_2)\text{H}^+$ as the major ion. No detectable signal existed for ions with exchangeable hydrogens. The ^1H in the formula originated from the proton-transfer reaction leading to ionization in the CIMS. If the product were instead a carboxylic acid, we would expect to observe $(\text{C}_6\text{D}_{15}\text{HO}_3\text{Si})\text{H}^+$. Further details regarding this experiment are in Section S3 of the Supporting Information.

The product distribution in the D4 and D5 oxidation experiments differed substantially from the D3 experiments. Monofunctional products, siloxanol and to a lesser extent formate ester, dominated the product signals. Additionally, the signal yields of siloxanol and formate ester showed little sensitivity to the RO_2 lifetime and reaction partner. In the D4 and D5 experiments, signals for $(\text{C}_8\text{H}_{23}\text{O}_7\text{Si}_4\text{N})\text{H}^+$ and

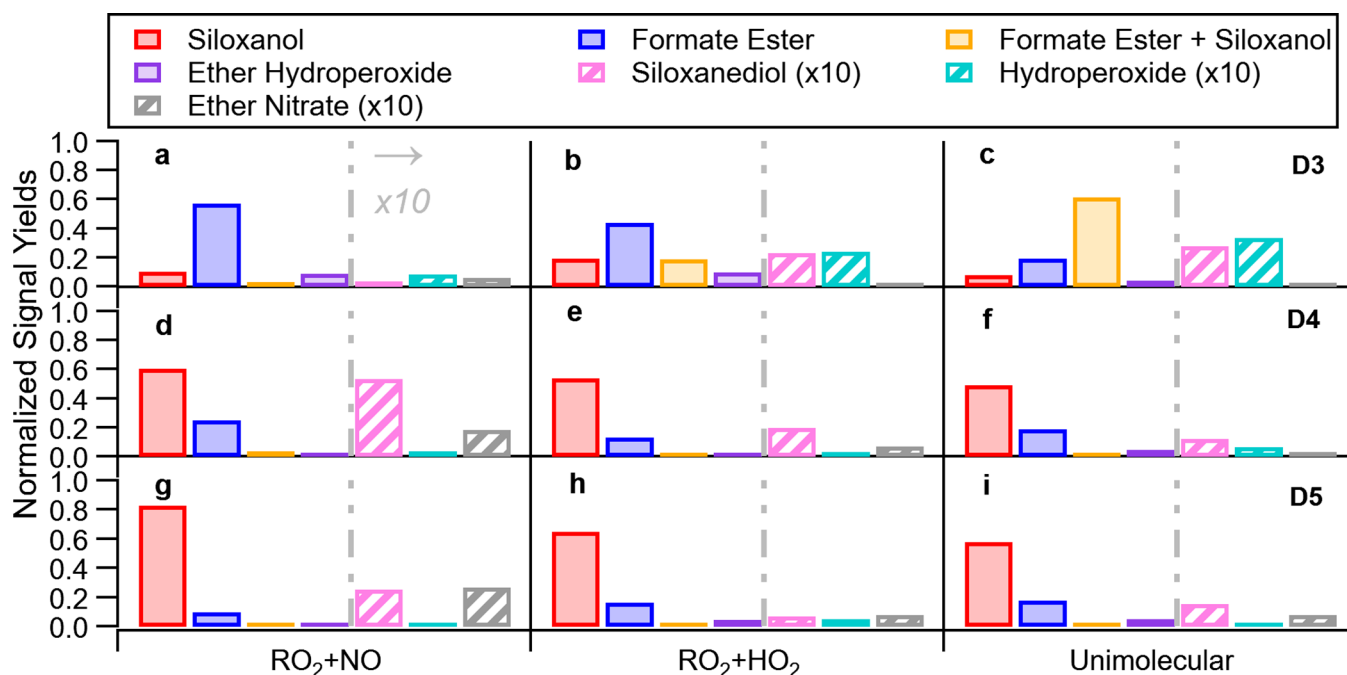
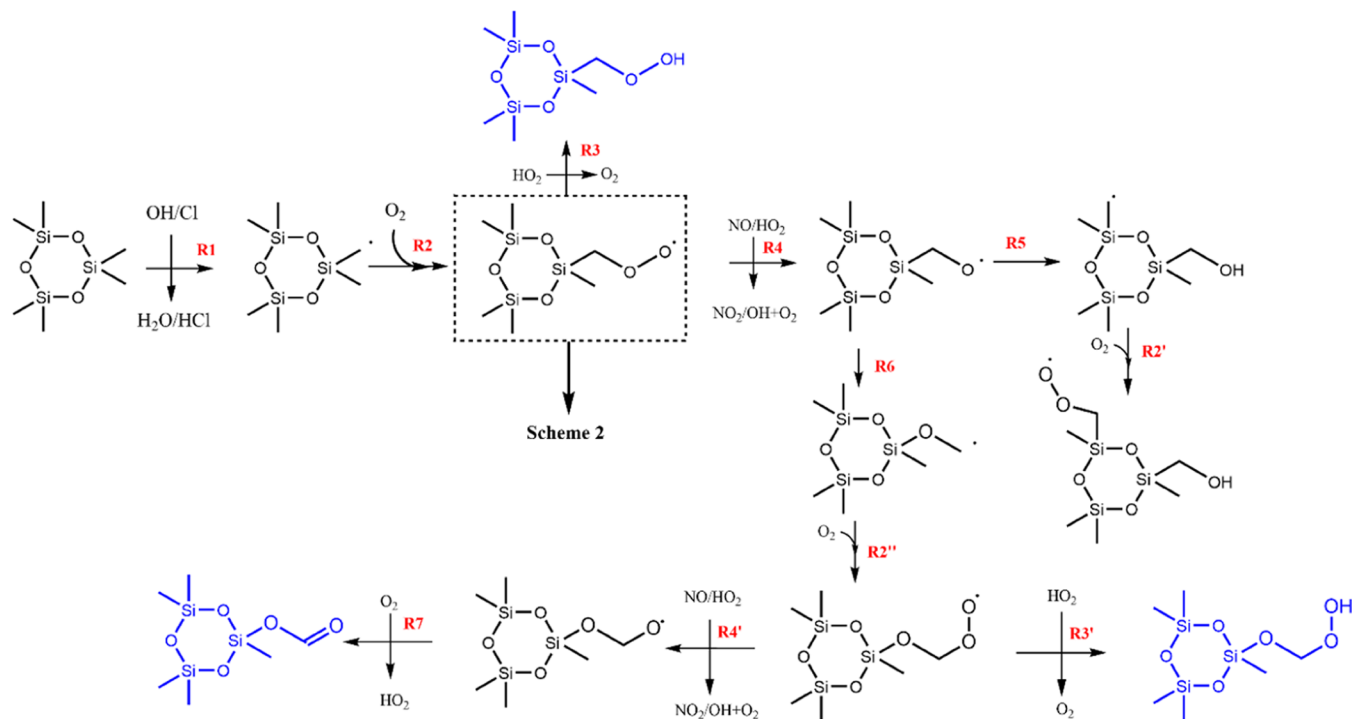


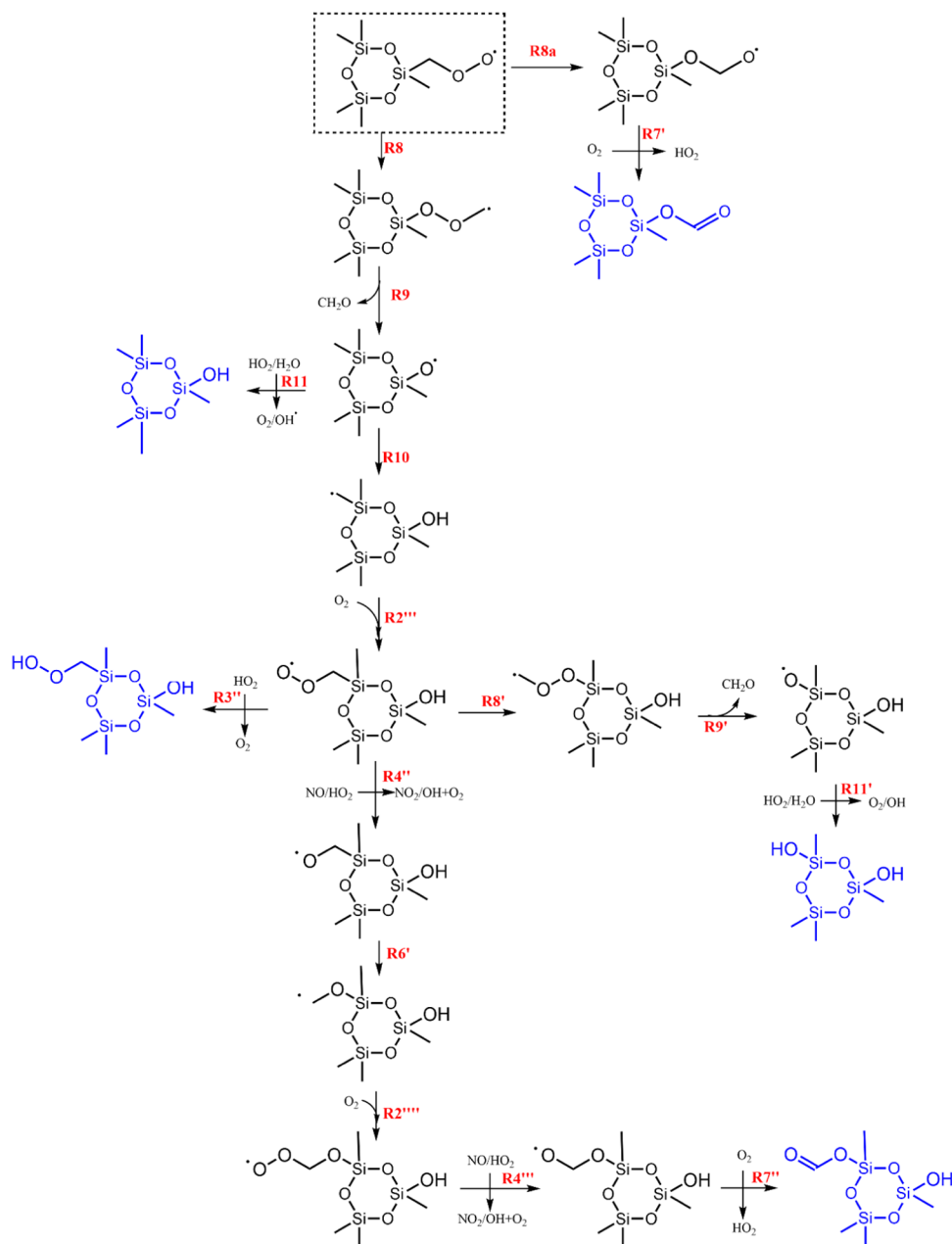
Figure 3. Signal yield of different cVMS oxidation products when RO₂ was most likely to react with (a, d, g) NO, (b, e, h) HO₂, or (c, f, i) when unimolecular reactions are favored, divided by the signal of the siloxane lost at that point. Panels (a–c) are for D3, (d–f) for D4, and (g–i) for D5 oxidation. The signals for siloxanediol, ether hydroperoxide, and ether nitrate are multiplied by 10 and striped for visual clarity.

Scheme 1. Potential Reactions of cVMS in High NO_x/HO₂ Conditions



(C₁₀H₂₉O₈Si₅N)⁺H⁺, attributed to the organic nitrates, and (C₈H₂₃O₈Si₄N)⁺H⁺ and (C₁₀H₂₉O₉Si₅N)⁺H⁺, attributed to the ether organic nitrates, were detected. However, these compounds appeared to be formed with significantly smaller yields than the siloxanol and formate ester products. Only the ether nitrate yields are shown in Figure 3. Proton-transfer ionization can lead to fragmentation of organic nitrates through nitric acid loss. As a result, instrument response for

the protonated organic nitrate can be low with high limits of detection. We detected the nitric acid loss fragment, (C₁₀H₂₈O₆Si₅)⁺H⁺, for the ether nitrate product at ~25% of the ether nitrate signal for D5, which suggests that some fragmentation did occur. We did not observe ions consistent with either water- or NO₂-loss fragmentation pathways or charge-transfer products. Although the reagent ion may be ineffective at detecting organic nitrates, we expect that the

Scheme 2. Potential Reactions of cVMS in Low NO_x/HO_2 Condition

yield of organic nitrates in these experiments was small given that both the organic nitrate signal and the total product signals were similar under the different RO_2 fates investigated, which ranged from 99% of RO_2 reacting with NO in the $\text{RO}_2 + \text{NO}$ conditions to $\sim 5\%$ reacting with NO in the $\text{RO}_2 + \text{HO}_2$ experiments. More discussion on the instrument response is in Section S4 of the Supporting Information. Additionally, previous work suggests that organic nitrate yields are low. Organic nitrates have not been detected before this work, even when cVMS was oxidized under high NO conditions.^{4,18} Carter et al.⁵³ performed environmental chamber experiments investigating how siloxanes alter ozone formation in high NO_x conditions. Through a model-measurement comparison, they determined that their results were inconsistent with organic nitrate formation; however, siloxane oxidation products were not measured.

In works that identified products with an increased number of silicon atoms, $\text{RO}_2 + \text{RO}_2$ reactions or reactions within the condensed phase likely occurred. In our experiments, $\text{RO}_2 + \text{RO}_2$ reactions were minimal under all conditions ($< 1\%$) and no aerosol was formed; thus, we did not expect to observe products with an increased number of silicon atoms.

3.2. Discussion of the Reaction Mechanism

In most previous studies, the major oxidation products have typically been attributed to siloxanol and formate ester, though formate ester has only been detected experimentally twice.^{4,5} The siloxanol has been suggested to be a hydrolysis product of formate ester.⁴ Other works have suggested unusual reactions that could potentially explain the formation of the siloxanol and the formate ester products,^{8,36,37} however, a lack of controlled and varied RO_2 fates in these experiments prevents a comprehensive assessment of the mechanism. In this work,

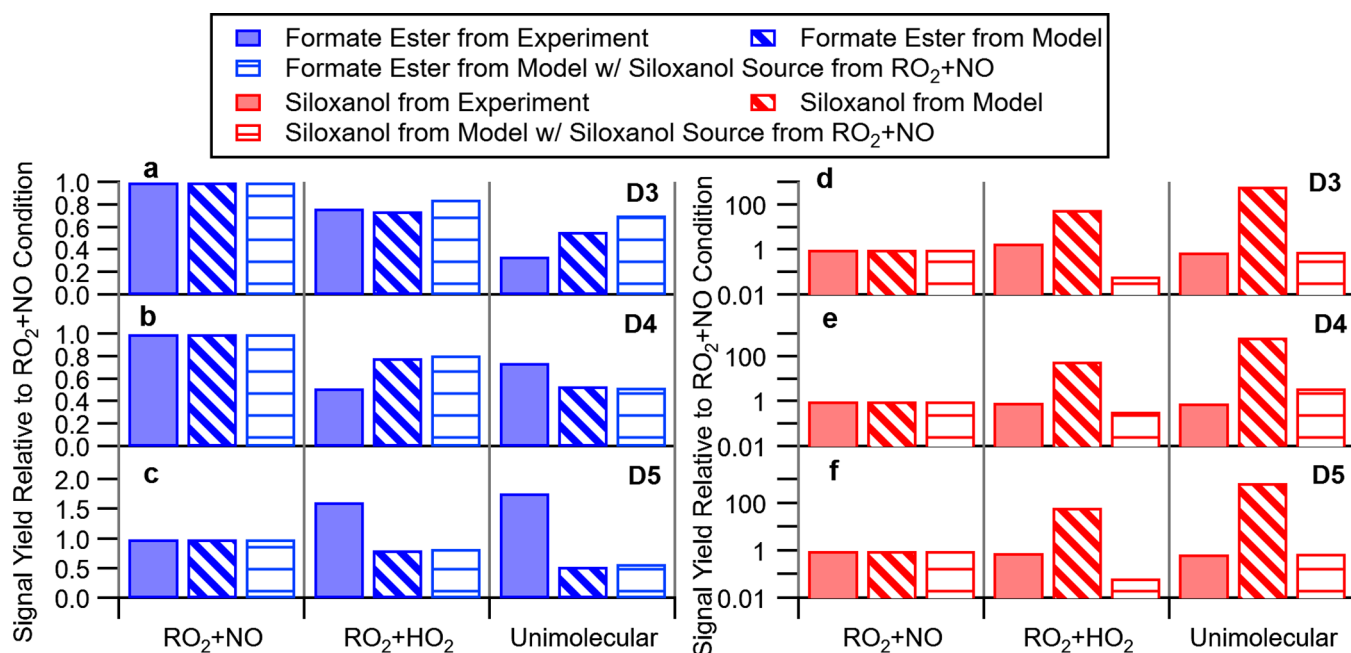


Figure 4. Signal yields of formate ester (a–c) and siloxanol (d–f) for all three cVMS from the experimental results and kinetic modeling using the mechanism presented, normalized to the results from the $\text{RO}_2 + \text{NO}$ conditions. Panels (a) and (d) are for D3 oxidation, (b) and (e) are for D4 oxidation, and (c) and (f) for D5. Note the log axis on siloxanol results. Only the rate constants for reactions with OH/Cl and wall loss constants were changed between cVMS. In the model results that had a source of siloxanol from the $\text{RO}_2 + \text{NO}$ reaction, 5% of the reaction product made siloxanol directly, and the other 95% made RO.

we varied the lifetime and reaction partner of the RO_2 radical to gain insight into these reactions. Additionally, our real-time measurement technique has the advantage that conversion of formate ester to siloxanol on surfaces will be minimized. In this section, we discuss the potential cVMS oxidation mechanism as compiled from previous experimental and theoretical studies.^{4,8,18,36,37} The schemes presented in this section are based on these previously proposed reactions as well as typical oxidation pathways in the atmosphere. In the following section, we implement the reaction mechanism in a zero-dimensional kinetic box model and compare it to our measurements.

3.2.1. $\text{RO}_2 + \text{NO}$. As shown in Scheme 1, cVMS oxidation is initiated by OH or Cl abstracting a hydrogen from one of the methyl groups (R1). The resulting alkyl radical quickly reacts with O_2 forming RO_2 (R2). When the NO/HO_2 ratio is greater than 2, such as urban locations, the primary reaction of RO_2 is with NO .⁴⁶ This reaction has two channels, one that forms an alkoxy radical (RO) and NO_2 (R4), and one that forms an organic nitrate ($-\text{ONO}_2$; not shown). Based on our measurements and as discussed in Section 3.1, we suggest that the organic nitrate channel is minor and that reaction with NO mainly proceeds through reaction R4. Possible fates for the $\text{R}_3\text{SiCH}_2\text{O}^\bullet$ radical include reaction with O_2 , decomposition, and isomerization. Isomerization reactions were expected to dominate as reactions with O_2 to form R_3SiCHO (not shown) and decomposition have been calculated to be at least 10 orders of magnitude slower than isomerization.³⁶ Possible isomerization pathways include a hydrogen shift from an adjacent methyl group or a unique rearrangement (R6) to form a carbon-based radical. R6 is inaccessible to carbon-based volatile organic compounds (VOCs). The calculated lifetime (from theoretically determined rate constants) for $\text{R}_3\text{SiCH}_2\text{O}^\bullet$ with respect to R6 was $\sim 6 \times 10^{-12}$ s for D3, and this isomerization is expected to be the major RO fate.³⁶ The most

intense hydroperoxide and nitrate signals detected during oxidation in this work are consistent with the formation of ether hydroperoxide and ether nitrate, consistent with R6 occurring rapidly. Note that the peroxy radicals formed from R5 followed by R2' and R6 followed by R2'' are isomers. However, based on theoretical calculations,³⁶ R5 is expected to be slow relative to R6, and thus, further reactions and products from R2' were not considered. The carbon-centered radical formed by R6, $\text{R}_3\text{SiOCH}_2^\bullet$, will subsequently add O_2 (R2'') to form a new ether peroxy radical.^{36,37} This radical can react with NO/HO_2 again (R4') to form an ether alkoxy radical. The formate ester forms when the ether alkoxy radical reacts with O_2 (R7). The ether peroxy radical can also react with HO_2 to form ether hydroperoxide (R3') or with NO to form ether nitrate (not shown).

3.2.2. $\text{RO}_2 + \text{HO}_2$. The main channel of the RO_2 reaction with HO_2 typically results in the formation of a hydroperoxide (R3).^{54,55} In our experiments, the observed intensity of this expected product was low. While this may be due to a low instrument response to hydroperoxides when using proton-transfer ionization, the fact that similar products in similar yields are formed under both $\text{RO}_2 + \text{NO}$ (<1% of RO_2 reacting with HO_2) and $\text{RO}_2 + \text{HO}_2$ (>90% of RO_2 reacting with HO_2) conditions leads us to suggest that RO_2 radicals can react with HO_2 to form the RO radical, OH, and O_2 (R4). The formation of the RO radical from the reaction of RO_2 with HO_2 has been observed previously in oxygenated organic molecules, leading to a radical recycling mechanism.^{55,56} Once R6 occurs, the reactions are the same in the NO case with the addition of R3' to form ether hydroperoxide.

3.2.3. Conditions Favoring Unimolecular Reactions. Under conditions of low HO_2 or NO concentrations, the lifetime of the RO_2 radical with respect to bimolecular reactions is long and unimolecular reactions may become

important. Possible unimolecular reactions of cVMS-derived RO_2 identified through quantum chemical calculations include 1,3-, 1,5-, and 1,7-hydrogen shifts to form QOOH with a propagated radical. However, the more favorable (lower energy barrier) isomerization was predicted to be the unusual pathway shown in R8 (Scheme 2).³⁶

After undergoing R8, the resulting radical is expected to quickly proceed through R9, generating a siloxy radical and formaldehyde. We suggest that the siloxy radical can undergo reaction R11 to make the siloxanol product after reaction with H_2O or HO_2 . The reaction of RO with H_2O (R11) has been proposed to occur on silica surfaces,⁵⁷ while Carter et al.⁵³ previously proposed the reaction of RO with HO_2 to make siloxanol. Fu et al.³⁶ suggested RO could undergo a reaction and abstract hydrogen from a methyl group on a nearby silicon atom (R10, 1,5 H-shift) or on the same silicon atom (1,3 H-shift), which is less favorable than the 1,5 H-shift. Both reactions propagate the radical to create another functional group on the cVMS molecule, and our measurement technique cannot distinguish which methyl groups have been modified; therefore, we did not consider this difference. Another unusual isomerization of the RO_2 radical (R8a) that was proposed initially by Atkinson et al.⁴ and used to explain observation of the formate ester product was previously investigated with quantum chemical calculations and determined to be energetically unfavorable.^{36,37}

3.3. Kinetic Model Using the Proposed Mechanism

We implement the reactions in Schemes 1 and 2, with rate constants informed from previously published quantum chemical calculations,³⁶ in a kinetic model (KinSim in Igor Pro) to investigate if the proposed mechanism can reproduce the changing intensity of different products under different RO_2 fates. The full mechanisms with rate constants for the three VMS studies are presented in Section S2 of the Supporting Information. Reactions to form organic nitrate with NO were excluded from the model. $\text{RO}_2 + \text{RO}_2$ reactions were minimal in all experiments (<0.5% of the RO_2 reactions were with another RO_2), and therefore were not considered in the mechanism. In the model, we held bimolecular reaction rates ($\text{RO}_2 + \text{HO}_2$ and $\text{RO}_2 + \text{NO}$) constant. As reaction R8a was previously determined to not be energetically favorable,³⁶ this reaction was not used. We included the oxidation of first-generation products with rate constants equal to the parent cVMS. As there is uncertainty in molar yields due to a lack of calibration standards, we focus on comparing the relative changes in signal yields as a function of RO_2 fate. Figure 4 shows the signal yields of the siloxanol and formate ester products from our experiments and the kinetic model at the point 10% of the cVMS was oxidized, normalized to the signal yield in the $\text{RO}_2 + \text{NO}$ conditions. By observing relative changes between the conditions, the absolute calibration of the oxidation products should not affect the interpretation of the data.

In our experiments with D3, we detect that the signal corresponding to the formate ester decreases with an increasing RO_2 lifetime, which is consistent with formate ester being formed after RO_2 reacts with NO/HO_2 . Consequently, the model captures this decrease albeit the measured decrease in formate ester yield with increasing RO_2 lifetime is greater than the decrease predicted by the model (Figure 4). For D5, we observed an increase in formate ester with increasing RO_2 lifetime, which contrasts with the model

prediction of a decreasing trend. The model also fails to capture the trends in the relative siloxanol yield for all three cVMS species; the model predicts an increase in siloxanol yield with increasing RO_2 lifetime, while the measurements suggest that the siloxanol yield is essentially independent of RO_2 lifetime and fate. In fact, the model predicts negligible siloxanol yield under $\text{RO}_2 + \text{NO}$ conditions (Figure S5), which causes the modeled siloxanol yield normalized to $\text{RO}_2 + \text{NO}$ conditions to change by orders of magnitude as the RO_2 lifetime increases. The model also predicts significantly less siloxanol ($\sim 100 \times$ less) formation than in our experiments, if we assume that we detect all of the products with equal sensitivity. Siloxanol formation has previously been attributed to hydrolysis of formate ester prior investigations of siloxane chemistry.^{4,7,18} Our high time-resolution measurements of formate ester and siloxanol are inconsistent with this hypothesis since we observed the simultaneous formation of both formate ester and siloxanol.

The model-measurement gap could potentially be explained by an unknown formation mechanism of siloxanol in high NO/HO_2 conditions. As a thought experiment, if a branching ratio is added to produce 5% of siloxanol and 95% of the RO after the reaction of RO_2 with NO, then the amount of siloxanol formed between experiments is slightly closer to the experimental results, though it underestimates the siloxanol formation in the $\text{RO}_2 + \text{HO}_2$ conditions (Figure 4). This formation of siloxanol could be achieved through a process such as the decomposition of a chemically activated alkoxy radical. Another possibility would be to have a faster rate constant for the isomerization in R8, as the siloxy radical formed after that isomerization could be a source of siloxanol. However, for this reaction to be important in all conditions (as the siloxanol is the largest product in high NO_x experiments with D4 and D5), the rate constant would need to be increased by multiple orders of magnitude to compete with the $\text{RO}_2 + \text{NO}$ reaction. Overall, the siloxanol formation mechanism remains unclear and more investigation to better understand why RO_2 fates do not significantly affect the products formed from D4 and D5 oxidation is required.

The model also fails to accurately capture the evolution of the largest product in the conditions that favor unimolecular reactions from D3 oxidation: the formate ester and siloxanol difunctional product (not shown in Figure 4). Because this difunctional product was the largest signal during the conditions that favor unimolecular reactions, it was anticipated that D3 $\text{R}_3\text{SiO}^\bullet$ radicals can readily undergo the auto-oxidation reaction shown in R10 after being formed from R8 and R9. Since siloxanol was formed in R10, the next steps need to preferentially make formate ester over another siloxanol. Therefore, R4'' needs to dominate over R8', though to form the initial siloxanol, R8 needs to dominate over R4. This pathway requires that the ratio of the R4:R8 rate constants is less than R4'':R8', which stands in contrast to theoretical calculations, suggesting that the isomerization rate increases as the molecules become more functionalized.³⁶ However, we did not detect any evidence in these experiments of the siloxanetriol product, which would likely be formed if the isomerization reactions R8 and R8' both dominated over bimolecular reactions, as the next RO_2 isomerization branching would likely not be different. Another possible explanation is that concentrations of NO or HO_2 were higher later in the experiment, pushing the mechanism down R4''. The model,

however, indicates that NO and HO₂ concentrations do not change enough to alter the product distribution.

Overall, it is evident that the oxidation mechanism is unable to replicate our experimental results, particularly for D4 and D5. The finding that D3 oxidation produces different products than D4 and D5 suggests that results, either from laboratory-based experiments or theoretical calculations, from smaller VMS and Si-containing molecules (i.e., D3, hexamethyldisiloxane [L2], and tetramethylsilane) may not hold for larger Si compounds. In particular, the lack of sensitivity on the oxidation product yields on RO₂ fate for D4 and D5 is unusual. As siloxanol was the most abundant product for D4 and D5 under all conditions, our results suggest that there is more unique chemistry occurring that requires further investigation.

3.4. Possible Fates of the First-Generation Products

As cVMS are globally distributed due to their long atmospheric lifetimes, their oxidation products will also be globally distributed. Previous research has focused on the parent compounds, though the oxidation products should not be discounted. Here, we use various structure–activity relationships (SAR) to investigate possible loss pathways for the main cVMS oxidation products we measured and discussed (siloxanol, formate ester, multisubstituted siloxanols/formate esters, hydroperoxides, and organic nitrates). The estimated values of vapor pressure, water solubility, and Henry's solubility (M atm⁻¹) constants of all of the products are presented in Table S6 of the Supporting Information.⁵⁸ Note that the Henry's law constant (atm M⁻¹) is the inverse of the Henry solubility.

Using the estimated vapor pressures, and assuming that absorption into organic aerosol is the main gas-particle partitioning method for these compounds, less than 1% of the least volatile oxidation product (the D5 siloxanediol) mass would partition to aerosol at a moderate organic aerosol loading of 10 μg m⁻³.⁵⁹ This value was determined using the vapor pressure estimated by MPBPWIN, which predicts vapor pressures about 1 order of magnitude lower than TEST, thus giving an upper limit to aerosol partitioning. It has been determined that cVMS heterogeneous reactions with components of mineral dust aerosol can lead to significant removal of the cVMS and its oxidation products, but due to the low typical dust loadings, the total loss to dust is expected to be minimal.³²

The oxidation products have estimated Henry's solubility constants that can be up to ~8 orders of magnitude higher (higher partitioning into the aqueous phase) than the parent cVMS. Out of the various methods compared, HenryWIN gave the largest estimated Henry's solubility coefficient of ~10⁵ M atm⁻¹ for the D3 siloxanediol. Even using this Henry's solubility constant, at most 30% of the siloxanediol will partition to cloud droplets, while there is no significant partitioning into an aqueous aerosol, as shown in Figure 5, adapted from Daumit et al.⁶⁰ We note that this estimate is uncertain as Henry's solubility and law constants measured in the laboratory vary by orders of magnitude between studies for the parent cVMS,⁶¹ and the Henry's law constants of the different oxidation products have not been measured.^{58,62,63} However, as we use the most extreme values from the structure–activity relationships, we assume these to be the upper limits for partitioning and thus conclude that absorptive and aqueous partitioning will have minor impacts on the mixing ratios of the oxidation products.

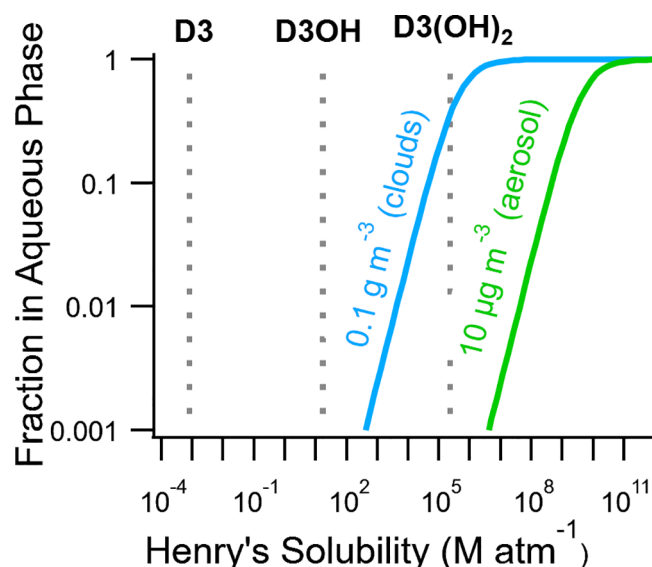


Figure 5. Estimated Henry's solubility, estimated with HenryWIN v3.21, for D3 and the siloxanol oxidation products (dashed lines). The mass concentration labels on the solid lines correspond to the amount of liquid water in clouds or ambient aerosol. Only siloxanol products are shown as the hydroxyl groups change the Henry's solubility most significantly. Larger cVMS oxidation products are estimated to have lower Henry's solubility than D3. All values are listed in Table S6 of the Supporting Information. Adapted with permission from Daumit, K. E.; Carrasquillo, A. J.; Hunter, J. F.; Kröll, J. H. Laboratory Studies of the Aqueous-Phase Oxidation of Polyols: Submicron Particles vs Bulk Aqueous Solution. *Atmos. Chem. Phys.* 2014, 14 (19), 10773–10784. <https://doi.org/10.5194/acp-14-10773-2014>.

The oxidized products may also be transformed in the atmosphere via oxidation. Atkinson et al.⁴ measured the rate constants of tetramethylsilane and trimethylsiloxanol reactions with Cl atoms and OH radicals, which showed that the rate constant for the siloxanol oxidation reactions were 2 times faster than the parent compounds for Cl and 10 times faster for OH. However, it is uncertain how the rate constants will change with larger cVMS. Using the Atmospheric Oxidation Program for Microsoft Windows (AOPWIN) in EPIWIN with the adjustments to Si-containing group contributions suggested by Alton and Browne (2020),⁵ the rate constant for reaction with OH is estimated to be approximately a factor of 5 times faster for D3OH compared to D3, and 3 times faster for D5OH compared to D5. This lowers the lifetime of D3OH and D5OH to approximately 2 days for both of the products, compared to 11 and 4.4 days.⁵ Based on this work, it is probable that, like the parent VMS compounds, these first-generation oxidation products will have atmospheric lifetimes of days, and thus, it is necessary to better understand multiple-generation oxidation products and their potential chemistry and deposition to completely understand cVMS environmental fates.

4. CONCLUSIONS

As ~90% of cVMS emitted into the environment partitions into the atmosphere,³ understanding the atmospheric degradation of these compounds is critical for understanding their environmental impacts. In this work, we oxidized three cVMS under conditions of different RO₂ fates and measured the oxidation products to gain insight into the cVMS oxidation mechanism. We observed that the main oxidation product for

D4 and D5 is siloxanol, regardless of the fate of the peroxy radical. As D4 and D5 are the most abundant cVMS in the atmosphere, we suggest that in chemical transport models cVMS oxidation products can be adequately represented as siloxanol, similar to previous representations of this chemistry.³⁰ Due to the high vapor pressure and low water solubility of the cVMS and oxidation products, it is predicted that not only is the parent cVMS globally distributed,^{13,64} the oxidation products are likely also globally present, requiring multiple generations of oxidation before significant removal will occur. Because the oxidation products are also likely to be long lived in the atmosphere, more measurements of the oxidation products in the atmosphere and environmental matrices are necessary to better understand the environmental processing of these anthropogenic chemicals.

■ ASSOCIATED CONTENT

SI Supporting Information

The Supporting Information is available free of charge at <https://pubs.acs.org/doi/10.1021/acsenvironau.1c00043>.

Detailed information of the peak fitting in TOFWARE, KinSim mechanism and inputs, isotopically labeled D₁₈L2 oxidation experiment, instrument response in different conditions, and the estimated physical parameters of cVMS and the oxidation products (PDF)

■ AUTHOR INFORMATION

Corresponding Author

Eleanor C. Browne – Department of Chemistry, University of Colorado, Boulder, Colorado 80309, United States; Cooperative Institute for Research in Environmental Sciences, University of Colorado, Boulder, Colorado 80309, United States; orcid.org/0000-0002-8076-9455; Phone: 303-735-7685; Email: Eleanor.Browne@Colorado.edu

Author

Mitchell W. Alton – Department of Chemistry, University of Colorado, Boulder, Colorado 80309, United States; Cooperative Institute for Research in Environmental Sciences, University of Colorado, Boulder, Colorado 80309, United States; orcid.org/0000-0002-7119-3706

Complete contact information is available at: <https://pubs.acs.org/10.1021/acsenvironau.1c00043>

Author Contributions

M.W.A. and E.C.B. designed the experiments. M.W.A. performed all of the experiments that contributed to this work. The analysis of the data was performed mainly by M.W.A. with support and guidance from E.C.B. The manuscript was written through the contributions of both authors. Both authors have given approval to the final version of the manuscript.

Notes

The authors declare no competing financial interest. The experimental data is publicly available through the Index of Chamber Atmospheric Research in the United States website (<https://icarus.ucdavis.edu/experimentset/242>, <https://icarus.ucdavis.edu/experimentset/243>, <https://icarus.ucdavis.edu/experimentset/244>).

Caution! Ultraviolet light is damaging to biological tissues. Caution is required when working with any lights that emit

ultraviolet wavelengths, and protective eyewear must be used at all times.

■ ACKNOWLEDGMENTS

This research was supported by the National Science Foundation under Grant CHE-1808606. Additional funding to support MWA was provided by the Cooperative Institute for Research in Environmental Sciences Graduate Student Research Fellowship Grant.

■ REFERENCES

- (1) Organisation for Economic Co-Operation and Development. *The 2004 OECD List of High Production Volume Chemicals*; OECD, 2004.
- (2) U.S. Environmental Protection Agency. CompTox Chemicals Dashboard, 2021. <https://comptox.epa.gov/dashboard/DTXSID102718>.
- (3) Mackay, D.; Cowan-Ellsberry, C. E.; Powell, D. E.; Woodburn, K. B.; Xu, S.; Kozerski, G. E.; Kim, J. Decamethylcyclopentasiloxane (D5) Environmental Sources, Fate, Transport, and Routes of Exposure. *Environ. Toxicol. Chem.* **2015**, *34*, 2689–2702.
- (4) Atkinson, R.; Tuazon, E. C.; Kwok, E. S. C.; Arey, J.; Aschmann, S. M.; Bridier, I. Kinetics and Products of the Gas-Phase Reactions of (CH₃)₄Si, (CH₃)₃SiCH₂OH, (CH₃)₃SiOSi(CH₃)₃ and (CD₃)₃SiOSi(CD₃)₃ with Cl Atoms and OH Radicals. *J. Chem. Soc. Faraday Trans.* **1995**, *91*, No. 3033.
- (5) Alton, M. W.; Browne, E. C. Atmospheric Chemistry of Volatile Methyl Siloxanes: Kinetics and Products of Oxidation by OH Radicals and Cl Atoms. *Environ. Sci. Technol.* **2020**, *54*, 5992–5999.
- (6) Atkinson, R. Kinetics of the Gas-Phase Reactions of a Series of Organosilicon Compounds with Hydroxyl and Nitrate (NO₃) Radicals and Ozone at 297 +/- 2 K. *Environ. Sci. Technol.* **1991**, *25*, 863–866.
- (7) Markgraf, S. J.; Wells, J. R. The Hydroxyl Radical Reaction Rate Constants and Atmospheric Reaction Products of Three Siloxanes. *Int. J. Chem. Kinet.* **1997**, *29*, 445–451.
- (8) Sommerlade, R.; Parlar, H.; Wrobel, D.; Kochs, P. Product Analysis and Kinetics of the Gas-Phase Reactions of Selected Organosilicon Compounds with OH Radicals Using a Smog Chamber-Mass Spectrometer System. *Environ. Sci. Technol.* **1993**, *27*, 2435–2440.
- (9) Safron, A.; Strandell, M.; Kierkegaard, A.; Macleod, M. Rate Constants and Activation Energies for Gas-Phase Reactions of Three Cyclic Volatile Methyl Siloxanes with the Hydroxyl Radical. *Int. J. Chem. Kinet.* **2015**, *47*, 420–428.
- (10) Bernard, F.; Papanastasiou, D. K.; Papadimitriou, V. C.; Burkholder, J. B. Temperature Dependent Rate Coefficients for the Gas-Phase Reaction of the OH Radical with Linear (L2, L3) and Cyclic (D3, D4) Permethylsiloxanes. *J. Phys. Chem. A* **2018**, *122*, 4252–4264.
- (11) Kim, J.; Xu, S. Quantitative Structure-Reactivity Relationships of Hydroxyl Radical Rate Constants for Linear and Cyclic Volatile Methylsiloxanes. *Environ. Toxicol. Chem.* **2017**, *36*, 3240–3245.
- (12) Tuazon, E. C.; Aschmann, S. M.; Atkinson, R. Atmospheric Degradation of Volatile Methyl-Silicon Compounds. *Environ. Sci. Technol.* **2000**, *34*, 1970–1976.
- (13) Genualdi, S.; Harner, T.; Cheng, Y.; MacLeod, M.; Hansen, K. M.; Van Egmond, R.; Shoeib, M.; Lee, S. C. Global Distribution of Linear and Cyclic Volatile Methyl Siloxanes in Air. *Environ. Sci. Technol.* **2011**, *45*, 3349–3354.
- (14) Xu, S.; Warner, N.; Bohlin-Nizzetto, P.; Durham, J.; McNett, D. Long-Range Transport Potential and Atmospheric Persistence of Cyclic Volatile Methylsiloxanes Based on Global Measurements. *Chemosphere* **2019**, *228*, 460–468.
- (15) Warner, N. A.; Evenset, A.; Christensen, G.; Gabrielsen, G. W.; Borgä, K.; Leknes, H. Volatile Siloxanes in the European Arctic: Assessment of Sources and Spatial Distribution. *Environ. Sci. Technol.* **2010**, *44*, 7705–7710.

- (16) Brooke, D.; Crookes, M.; Gray, D.; Robertson, S. *Environmental Risk Assessment Report: Decamethylcyclopentasiloxane*; Environment Agency, 2009.
- (17) Brooke, D. N.; Brooke, M. J.; Gray, D.; Robertson, S.; Crookes, M.; Gray, D.; Robertson, S. *Environmental Risk Assessment Report: Octamethylcyclotetrasiloxane*; Environment Agency, 2009.
- (18) Allen, R. B.; Annelin, R. B.; Atkinson, R.; Carpenter, J. C.; Carter, W. L. P.; Chandra, G.; Fendinger, N. J.; Gerhards, R.; Grigoros, S.; Hatcher, J. A.; Hobson, J. F.; Kochs, P.; Lehmann, R. G.; Maxim, L. D.; Mazzoni, S. M.; Mihaich, E. M.; Miyakawa, Y.; Pohl, E. R.; Powell, D. E.; Roy, S.; Sawano, T.; Slater, G. S.; Spivack, J. L.; Stevens, C.; Wischer, D. Organosilicon Materials. In *The Handbook of Environmental Chemistry*; Chandra, G., Ed.; Springer: Berlin, Heidelberg, 1997; Vol. 3.
- (19) European Chemicals Agency. *Recommendation of the European Chemicals Agency of 20 December 2011 for the Inclusion of Substances in Annex XIV to REACH (List of Substances Subject to Authorisation) of Regulation (EC) No 1907/2006*; European Chemicals Agency, 2011; Vol. 1, pp 1–7.
- (20) United Kingdom Health & Safety Executive. *Annex XV Restriction Report Proposal for a Restriction*; United Kingdom Health & Safety Executive, 2015; pp 1–89.
- (21) European Chemicals Agency. *Recommendation of the European Chemicals Agency of 14 April 2021 for the Inclusion of Substances in Annex XIV to REACH (List of Substances Subject to Authorisation)*; EPA, 2021; Vol. 1, pp 1–7.
- (22) Wu, Y.; Johnston, M. V. Molecular Characterization of Secondary Aerosol from Oxidation of Cyclic Methylsiloxanes. *J. Am. Soc. Mass Spectrom.* **2016**, *27*, 402–409.
- (23) Yucuis, R. A.; Stanier, C. O.; Hornbuckle, K. C. Cyclic Siloxanes in Air, Including Identification of High Levels in Chicago and Distinct Diurnal Variation. *Chemosphere* **2013**, *92*, 905–910.
- (24) Milani, A.; Al-Naiema, I. M.; Stone, E. A. Detection of a Secondary Organic Aerosol Tracer Derived from Personal Care Products. *Atmos. Environ.* **2021**, *246*, No. 118078.
- (25) Ahrens, L.; Harner, T.; Shoeib, M. Temporal Variations of Cyclic and Linear Volatile Methylsiloxanes in the Atmosphere Using Passive Samplers and High-Volume Air Samplers. *Environ. Sci. Technol.* **2014**, *48*, 9374–9381.
- (26) Gallego, E.; Perales, J. F.; Roca, F. J.; Guardino, X.; Gadea, E. Volatile Methyl Siloxanes (VMS) Concentrations in Outdoor Air of Several Catalan Urban Areas. *Atmos. Environ.* **2017**, *155*, 108–118.
- (27) US EPA. *Enforceable Consent Agreement for Environmental Testing for Octamethylcyclotetrasiloxane (D4) (CASRN 556-67-2) Docket No. EPA-HQ-OPPT-2012-0209*; EPA, 2014.
- (28) Dudzina, T.; Von Goetz, N.; Bogdal, C.; Biesterbos, J. W. H.; Hungerbühler, K. Concentrations of Cyclic Volatile Methylsiloxanes in European Cosmetics and Personal Care Products: Prerequisite for Human and Environmental Exposure Assessment. *Environ. Int.* **2014**, *62*, 86–94.
- (29) Bzdek, B. R.; Horan, A. J.; Pennington, M. R.; Janecek, N. J.; Baek, J.; Stanier, C. O.; Johnston, M. V. Silicon Is a Frequent Component of Atmospheric Nanoparticles. *Environ. Sci. Technol.* **2014**, *48*, 11137–11145.
- (30) Janecek, N. J.; Hansen, K. M.; Stanier, C. O. Comprehensive Atmospheric Modeling of Reactive Cyclic Siloxanes and Their Oxidation Products. *Atmos. Chem. Phys.* **2017**, *17*, 8357–8370.
- (31) Chandramouli, B.; Kamens, R. M. The Photochemical Formation and Gas-Particle Partitioning of Oxidation Products of Decamethyl Cyclopentasiloxane and Decamethyl Tetrasiloxane in the Atmosphere. *Atmos. Environ.* **2001**, *35*, 87–95.
- (32) Navea, J. G.; Xu, S.; Stanier, C. O.; Young, M. A.; Grassian, V. H. Heterogeneous Uptake of Octamethylcyclotetrasiloxane (D4) and Decamethylcyclopentasiloxane (D5) onto Mineral Dust Aerosol under Variable RH Conditions. *Atmos. Environ.* **2009**, *43*, 4060–4069.
- (33) Janecek, N. J.; Marek, R. F.; Bryngelson, N.; Singh, A.; Bullard, R. L.; Brune, W. H.; Stanier, C. O. Physical Properties of Secondary Photochemical Aerosol from OH Oxidation of a Cyclic Siloxane. *Atmos. Chem. Phys.* **2019**, *19*, 1649–1664.
- (34) Fairbrother, A.; Woodburn, K. B. Assessing the Aquatic Risks of the Cyclic Volatile Methyl Siloxane D4. *Environ. Sci. Technol. Lett.* **2016**, *3*, 359–363.
- (35) Tang, X.; Misztal, P. K.; Nazaroff, W. W.; Goldstein, A. H. Siloxanes Are the Most Abundant Volatile Organic Compound Emitted from Engineering Students in a Classroom. *Environ. Sci. Technol. Lett.* **2015**, *2*, 303–307.
- (36) Fu, Z.; Xie, H.-B.; Elm, J.; Guo, X.; Fu, Z.; Chen, J. Formation of Low-Volatile Products and Unexpected High Formaldehyde Yield from the Atmospheric Oxidation of Methylsiloxanes. *Environ. Sci. Technol.* **2020**, *54*, 7136–7145.
- (37) Ren, Z.; da Silva, G. Auto-Oxidation of a Volatile Silicon Compound: A Theoretical Study of the Atmospheric Chemistry of Tetramethylsilane. *J. Phys. Chem. A* **2020**, *124*, 6544–6551.
- (38) Coggon, M. M.; McDonald, B. C.; Vlasenko, A.; Veres, P. R.; Bernard, F.; Koss, A. R.; Yuan, B.; Gilman, J. B.; Peischl, J.; Aikin, K. C.; DuRant, J.; Warneke, C.; Li, S.; de Gouw, J. A. Diurnal Variability and Emission Pattern of Decamethylcyclopentasiloxane (D5) from the Application of Personal Care Products in Two North American Cities. *Environ. Sci. Technol.* **2018**, *52*, S610–S618.
- (39) Tran, T. M.; Abualnaja, K. O.; Asimakopoulos, A. G.; Covaci, A.; Gevao, B.; Johnson-Restrepo, B.; Kumosani, T. A.; Malarvannan, G.; Minh, T. B.; Moon, H. B.; Nakata, H.; Sinha, R. K.; Kannan, K. A Survey of Cyclic and Linear Siloxanes in Indoor Dust and Their Implications for Human Exposures in Twelve Countries. *Environ. Int.* **2015**, *78*, 39–44.
- (40) Praske, E.; Otkjær, R. V.; Crounse, J. D.; Hethcox, J. C.; Stoltz, B. M.; Kjaergaard, H. G.; Wennberg, P. O. Atmospheric Autoxidation Is Increasingly Important in Urban and Suburban North America. *Proc. Natl. Acad. Sci. U.S.A.* **2018**, *115*, 64–69.
- (41) Wu, Y.; Johnston, M. V. Aerosol Formation from OH Oxidation of the Volatile Cyclic Methyl Siloxane (CVMS) Decamethylcyclopentasiloxane. *Environ. Sci. Technol.* **2017**, *51*, 4445–4451.
- (42) Cheng, Z.; Qiu, X.; Shi, X.; Zhu, T. Identification of Organosiloxanes in Ambient Fine Particulate Matters Using an Untargeted Strategy via Gas Chromatography and Time-of-Flight Mass Spectrometry. *Environ. Pollut.* **2021**, *271*, No. 116128.
- (43) Lu, D.; Tan, J.; Yang, X.; Sun, X.; Liu, Q.; Jiang, G.; Tan, J.; Sun, X.; Lu, D.; Jiang, G.; Yang, X. Unraveling the Role of Silicon in Atmospheric Aerosol Secondary Formation: A New Conservative Tracer for Aerosol Chemistry. *Atmos. Chem. Phys. Discuss.* **2018**, *19*, 2861–2870.
- (44) Lu, D.; Liu, Q.; Yu, M.; Yang, X.; Fu, Q.; Zhang, X.; Mu, Y.; Jiang, G. Natural Silicon Isotopic Signatures Reveal the Sources of Airborne Fine Particulate Matter. *Environ. Sci. Technol.* **2018**, *52*, 1088–1095.
- (45) Charan, S.; Huang, Y.; Buenconsejo, R.; Li, Q.; Cocker, D., III; Seinfeld, J. Secondary Organic Aerosol Formation from the Oxidation of Decamethylcyclopentasiloxane at Spherically Relevant OH Concentrations. *Atmos. Chem. Phys. Discuss.* **2021**, 917–928.
- (46) Ziemann, P. J.; Atkinson, R. Kinetics, Products, and Mechanisms of Secondary Organic Aerosol Formation. *Chem. Soc. Rev.* **2012**, *41*, 6582–6605.
- (47) Peng, Z.; Jimenez, J. L. KinSim: A Research-Grade, User-Friendly, Visual Kinetics Simulator for Chemical-Kinetics and Environmental-Chemistry Teaching. *J. Chem. Educ.* **2019**, *96*, 806–811.
- (48) Atkinson, R.; Baulch, D. L.; Cox, R. A.; Crowley, J. N.; Hampson, R. F.; Hynes, R. G.; Jenkin, M. E.; Rossi, M. J.; Troe, J. IUPAC Task Group on Atmospheric Chemical Kinetic Data Evaluation. *Atmos. Chem. Phys.* **2004**, *4*, 1461–1738.
- (49) Atkinson, R.; Baulch, D. L.; Cox, R. A.; Crowley, J. N.; Hampson, R. F.; Hynes, R. G.; Jenkin, M. E.; Rossi, M. J.; Troe, J. Evaluated Kinetic and Photochemical Data for Atmospheric Chemistry: Volume III—Gas Phase Reactions of Inorganic Halogens. *Atmos. Chem. Phys.* **2007**, *7*, 981–1191.
- (50) Liu, X.; Day, D. A.; Krechmer, J. E.; Brown, W.; Peng, Z.; Ziemann, P. J.; Jimenez, J. L. Direct Measurements of Semi-Volatile

Organic Compound Dynamics Show near-Unity Mass Accommodation Coefficients for Diverse Aerosols. *Commun. Chem.* **2019**, *2*, No. 98.

(51) Krechmer, J. E.; Pagonis, D.; Ziemann, P. J.; Jimenez, J. L. Quantification of Gas-Wall Partitioning in Teflon Environmental Chambers Using Rapid Bursts of Low-Volatility Oxidized Species Generated in Situ. *Environ. Sci. Technol.* **2016**, *50*, 5757–5765.

(52) Boethling, R.; Meylan, W. How Accurate Are Physical Property Estimation Programs for Organosilicon Compounds? *Environ. Toxicol. Chem.* **2013**, *8*, 2433–2440.

(53) Carter, W. L. P.; Pierce, J. A.; Malkina, I. L.; Luo, D. *Investigation of the Ozone Formation Potential of Selected Volatile Silicone Compounds*; Final Report to Dow Corning Corporation: Midland, MI, 1992.

(54) Seinfeld, J. H.; Pandis, S. N. *Atmospheric Chemistry and Physics: From Air Pollution to Climate Change*, 2nd ed.; John Wiley & Sons, Inc.: Hoboken, New Jersey, 2006.

(55) Orlando, J. J.; Tyndall, G. S. Laboratory Studies of Organic Peroxy Radical Chemistry: An Overview with Emphasis on Recent Issues of Atmospheric Significance. *Chem. Soc. Rev.* **2012**, *41*, 6294–6317.

(56) Jenkin, M. E.; Valorso, R.; Aumont, B.; Rickard, A. R. Estimation of Rate Coefficients and Branching Ratios for Reactions of Organic Peroxy Radicals for Use in Automated Mechanism Construction. *Atmos. Chem. Phys. Discuss.* **2019**, *19*, 7691–7717.

(57) Narayanasamy, J.; Kubicki, J. D. Mechanism of Hydroxyl Radical Generation from a Silica Surface: Molecular Orbital Calculations. *J. Phys. Chem. B* **2005**, *109*, 21796–21807.

(58) Xu, S.; Kropscott, B. Evaluation of the Three-Phase Equilibrium Method for Measuring Temperature Dependence of Internally Consistent Partition Coefficients (KOW, KOA, and KAW) for Volatile Methylsiloxanes and Trimethylsilanol. *Environ. Toxicol. Chem.* **2014**, *33*, 2702–2710.

(59) Donahue, N. M.; Robinson, A. L.; Pandis, S. N. Atmospheric Organic Particulate Matter: From Smoke to Secondary Organic Aerosol. *Atmos. Environ.* **2009**, *43*, 94–106.

(60) Daumit, K. E.; Carrasquillo, A. J.; Hunter, J. F.; Kroll, J. H. Laboratory Studies of the Aqueous-Phase Oxidation of Polyols: Submicron Particles vs. Bulk Aqueous Solution. *Atmos. Chem. Phys.* **2014**, *14*, 10773–10784.

(61) Sander, R. Compilation of Henry's Law Constants (Version 4.0) for Water as Solvent. *Atmos. Chem. Phys.* **2015**, *15*, 4399–4981.

(62) Xu, S.; Kozerski, G.; Mackay, D. Critical Review and Interpretation of Environmental Data for Volatile Methylsiloxanes: Partition Properties. *Environ. Sci. Technol.* **2014**, *48*, 11748–11759.

(63) Xu, S.; Kropscott, B. Method for Simultaneous Determination of Partition Coefficients for Cyclic Volatile Methylsiloxanes and Dimethylsilanediol. *Anal. Chem.* **2012**, *84*, 1948–1955.

(64) Krogseth, I. S.; Kierkegaard, A.; McLachlan, M. S.; Breivik, K.; Hansen, K. M.; Schlabach, M. Occurrence and Seasonality of Cyclic Volatile Methyl Siloxanes in Arctic Air. *Environ. Sci. Technol.* **2013**, *47*, 502–509.

Recommended by ACS

Reaction of OH with Aliphatic and Aromatic Isocyanates

Oliver Welz, Peter Deglmann, *et al.*

DECEMBER 08, 2022
THE JOURNAL OF PHYSICAL CHEMISTRY A

READ 

Comparison of the Yield and Chemical Composition of Secondary Organic Aerosol Generated from the OH and Cl Oxidation of Decamethylcyclopentasiloxane

Anita M. Avery, Andrew T. Lambe, *et al.*

JANUARY 05, 2023
ACS EARTH AND SPACE CHEMISTRY

READ 

Kinetics of Aldehyde Flavorant-Acetal Formation in E-Liquids with Different E-Cigarette Solvents and Common Additives Studied by ¹H NMR Spectroscopy

Paul J. Kerber and David H. Peyton

JULY 13, 2022
CHEMICAL RESEARCH IN TOXICOLOGY

READ 

Plastic Burning Impacts on Atmospheric Fine Particulate Matter at Urban and Rural Sites in the USA and Bangladesh

Md. Robiul Islam, Elizabeth A. Stone, *et al.*

JUNE 09, 2022
ACS ENVIRONMENTAL AU

READ 

Get More Suggestions >